Colloid and Surface Science
2017; 2(1): 26-36
http://www.sciencepublishinggroup.com/j/css
doi: 10.11648/j.css.20170201.14

Surface Characterization of Plasma Immersion Nitrogen Ion Implanted Austenitic Stainless Steel

Pandurangan Saravanan[1], Vngaranahalli Srinivasan Raja[2]

[1]R&D Center for Iron and Steel, Steel Authority of India Limited, Ranchi, India

[2]Department of Metallurgical Engineering and Materials Science, Indian Institute of Technology Bombay, Mumbai, India

Email address:
sarvan@sail-rdcis.com (P. Saravanan)

To cite this article:
Pandurangan Saravanan, Vngaranahalli Srinivasan Raja. Surface Characterization of Plasma Immersion Nitrogen Ion Implanted Austenitic Stainless Steel. *Colloid and Surface Science.* Vol. 2, No. 1, 2017, pp. 26-36. doi: 10.11648/j.css.20170201.14

Received: November 29, 2016; **Accepted**: January 3, 2017; **Published**: January 31, 2017

Abstract: Plasma immersion ion implantation (PIII) of nitrogen has been performed on three austenitic stainless steels namely, Type 304L SS, MnSS-1 (16%Cr-6%Mn-4Ni) and MnSS-2 (16%Cr-9%Mn) with at three different temperatures namely, 250, 380 and 500°C for 3 h. The GXRD studies shows that mixed iron nitride phases were formed along with expanded austenitic, when sample implanted at 250°C and 380°C. These nitrides are with different stoichiometry along the thickness and their formation is less favorable in nickel free Mn alloy at lower implantation temperature and timing (250°C for 3 h). On higher implantation condition (500°C, 6 h), Ni promotes the α′ formation and Mn suppress the α′ formation. Microhardness measurements revealed a significant increase in hardness after PIII treatment for all the alloys under investigation, but it is more effective in Ni free Mn containing SS.

Keywords: Plasma Immersion Ion Implantation, XRD, GXRD, Hardness

1. Introduction

Most of research in austenitic stainless steel continues to generate new ideas for improving mechanical and corrosion properties of this important class of engineering materials. The addition of nitrogen to these steels was made to improve corrosion resistance and wear properties [1-4]. Since corrosion and wear properties primarily concerns with its surface, surface modification has become viable route to improve this properties [5].

Out of most surface modification technique Plasma immersion ion implantation (PIII) developed by Conard et al.[6]which involves both the implantation and diffusion of nitrogen, seems toin the temperature range 250 – 500°C for stainless steels [1, 2, 4, 7-13]. This improvement was brought out by the phases formed on the surface the alloys as a result of PIII.The phases formed by PIII are called as expansion in austenite [1, 14]. While few others reported that it can lead to some iron nitrides like Fe_4N, Fe_2N, FeN etc., [15]. The phase formation in austenitic stainless steels due to N implantation is still unclear. It is well known fact that nitride formation mainly depends on the solubility of nitrogen in the metal matrix. It is known that the solubility of N in austenitic stainless steel, in general, depends on its alloying elements as well [16, 17]. Since it is known that the solubility of N in austenitic stainless steels can be increased by addition Mn in stainless steels in comparison with Ni, here we have undertaken a systematic study on the effect of Mn, and Ni on the phase formation on austenitic stainless steels under various N implanted conditions.

2. Experimental Work

2.1. Materials

Table 1. *Composition (wt%) of the austenitic stainless steels alloys.*

Material	Elements									
	C	Mn	S	P	Si	Ni	N	Cr	Mo	Cu
Type 304L	0.03	2.0	0.03	0.045	0.75	8.2	0.01	18.0	---	---
MnSS-1	0.06	6.15	0.009	0.05	0.36	4.17	0.08	16.45	0.07	1.0
MnSS-2	0.01	9.15	0.009	0.062	0.34	1.04	0.16	16.07	0.09	1-2

The effect of Ni and Mn on PIII treatment was studied by comparing three austenitic stainless steels namely, Type 304L

SS (18%Cr-8%Ni SS), MnSS-1(16%Cr-6%Mn-4%Ni SS) and MnSS-2 (16%Cr-9%Mn SS) their chemical composition are show in Table-1

2.2. Plasma Immersion Ion Implantation (PIII) Procedures

For plasma immersion ion implantation the samples were polished systematically using silicon carbide emery papers starting from 120 to 4/0 grade and finally using alumina powder of 0.25 μm. The plasma was produced by impact ionization of the operating gas by energetic electrons. These electrons are produced by thermoionic emission from hot tungsten filaments. The experimental set-up for PIII comprises a vacuum chamber and associated pumping systems, a substrate holder and heater, a plasma source and a high-voltage pulsed power supply. At the center of the vacuum chamber was kept a substrate holder usually in forms a disc. Below the substrate holder, a heater was kept connected to a 1:1 ratio transformer. The system was pumped to a base pressure of $7.0x10^{-6}$ Torr. From this the operating pressure of 10^{-4} Torr was achieved by introducing nitrogen in to the system. An electrically isolated thermocouple was used for measuring substrate temperature. Before the start of implantation, the surface oxide layer was removed by sputtering with argon gas for 30min.The substrate was negatively biased to a voltage of 1keV, and the implantation was done at 100 mA current with the dosage of 1.8 X 10^{19} ions/cm^2 for 3 h. The implantation was carried out for the same current density with the dose 3.6 x 10^{19}/cm^2 for 6h. The nitrogen implantation was also carried out at three different temperatures such as 250°C, 380°C and 500°C.

2.3. X-ray Diffraction

The phases formed on the surface of implanted samples were characterized by X-ray diffraction using an Expertpro diffractometer with CuKα radiation (λ = 1.54 A°) as a source. The diffractorgrams were scanned from 30 to 100°.

In order to know the phase change only at the surface due to PIII, implanted samples was examined using Glancing angle X-ray diffraction with a glancing angle of 2^0. The diffractorgrams were scanned from 30 to 100^0 using Expertpro diffractometer with CuKα radiation (λ = 1.54 A^0) as a source. The possible changes occurring in the phases formed at the surface of the alloys due to nitrogen implantation treatment were investigated by comparing diffractograms of the implanted samples with those of the untreated samples.

2.4. Surface Hardness

Load dependent surface microhardness testing was carried out on both the untreated and nitrogen implanted samples using Leica Vickers indentor (VMHT 10) microhardness tester with the load ranging from 15 to 300g.The hardness of the implanted alloys was compared with that of the untreated alloys to examine the effect of the implantation process on the microhardness characteristics of the alloys.

3. Results and Discussion

3.1. Phase Analysis

The XRD and GXRD pattern of the nitrogen implanted specimen surface appears to be different from that of the untreated Type 304L SS specimen Figure 1(a and b). The specimen on implantation displays a multiphase structure in the surface layer depending upon the implantation temperature. It is observed that the transformed ferrite/martensite peak $\alpha'_{(110)}$ disappears at 250°C and 380°C. The formation of α′ might be due to mechanical strain occurred during standard metallographic sample preparation prior to GXRD analysis [15, 18]. The α′ disappears with nitrogen ion implantation at 250°C and 380°C, stabilizing the fcc phase [19]. It is clearly seen in GXRD (Figure 1b) that nitrogen when implanted at 250°C suppresses the transformed ferrite/martensite and stabilises austenite phase, which is consistent with the results reported earlier [6]. Similar behavior of disappearance and reappearance of transformed ferrite/martensite peak $\alpha'_{(110)}$ were seen for MnSS-1 and MnSS-2 alloys (Figs.2 and 3).

3.1.1. Effect of Implantation Temperatures

XRD and GXRD patterns (Figure 1) of the nitrogen implanted specimens (250°C) showed two new broad peaks just ahead of $(111)_\gamma$ and $(200)_\gamma$ planes of the austenite, which may indicate the formation of a new phase. It was observed that the new phase peaks appear at lower angles as compared with those of $(111)_\gamma$ and $(200)_\gamma$ planes of austenite phase. Similar peaks were observed by other investigators previously and were considered to be due to interaction of nitrogen with the alloy matrix [20- 24]. Several possibilities have been suggested for nitrogen interaction with the alloy Dearnley et al., [25] in Plasma glow discharge, Ichii et al., [26], in Ion nitriding and Menthe et al, [27] in plasma nitriding). Some authors have indicated expansion of austenite lattice [20, 23, 24], while Haen et al., [28] reported the formation of different types of nitrides such as FeN, γ'-Fe_4N, Fe_3NiN in Type 304L SS due to Nitriding.

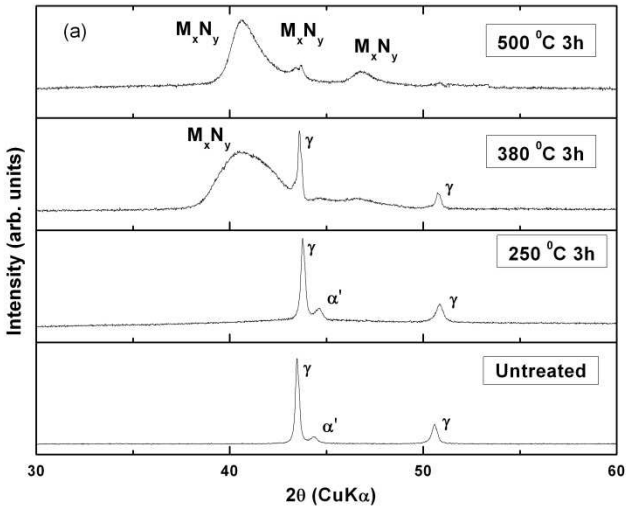

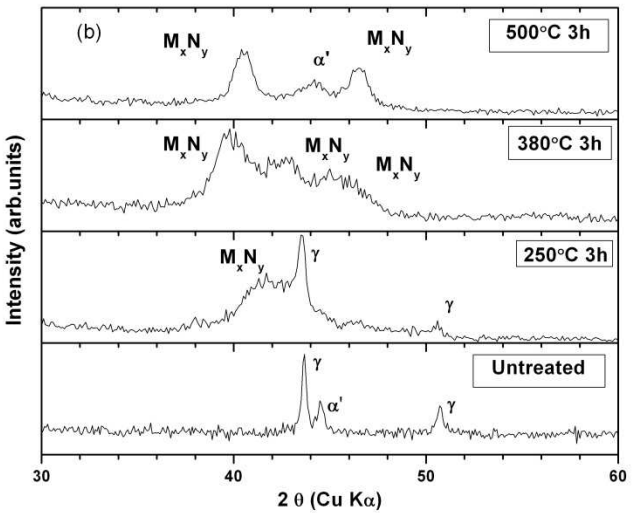

Figure 1. *Phase analysis of Type 304L SS after 3h PIII treated at 250°C, 380°C and 500°C a) XRD b) GXRD.*

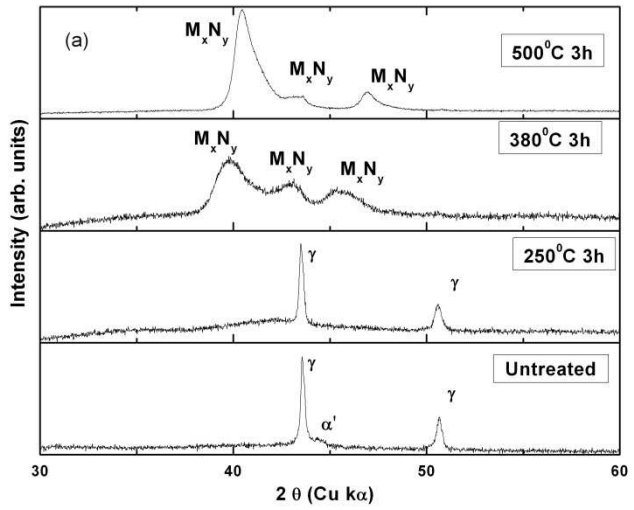

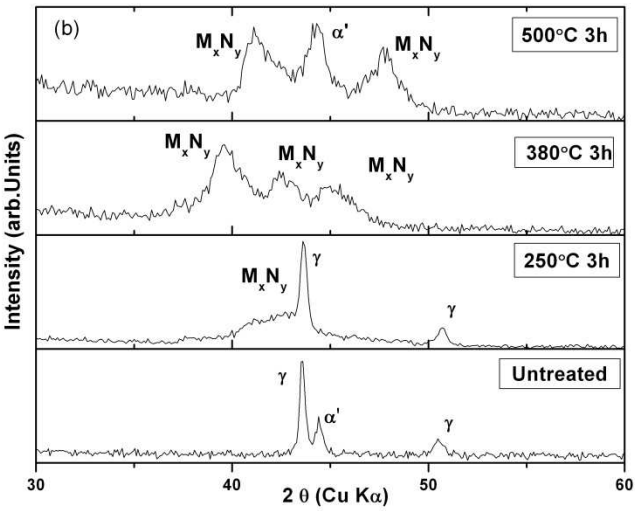

Figure 2. *Phase analysis of MnSS-1 after 3h PIII treated at 250°C, 380°C and 500°C a) XRD b) GXRD.*

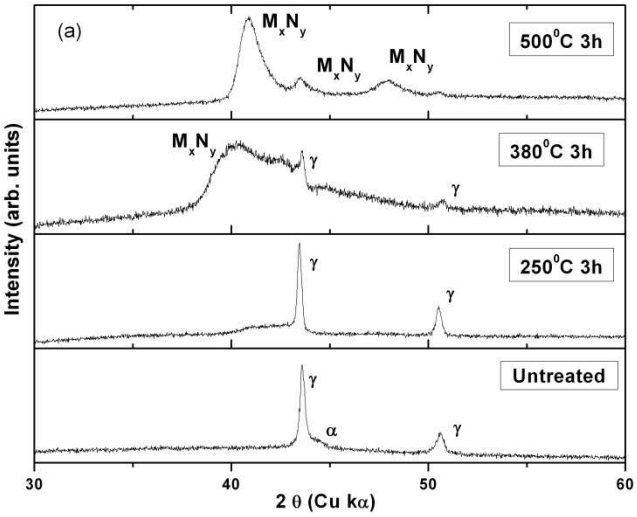

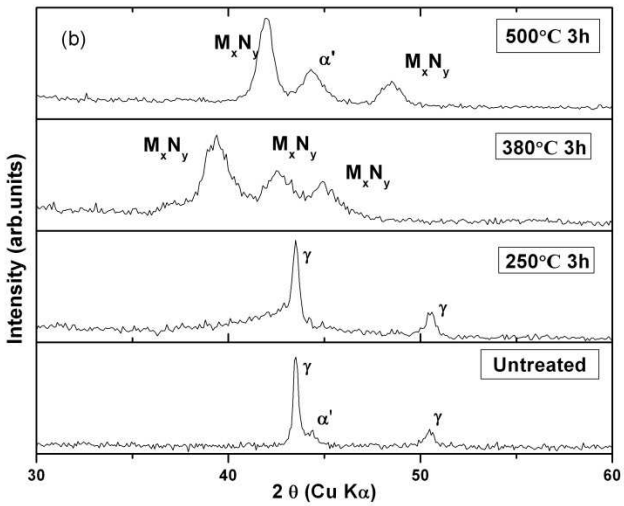

Figure 3. *Phase analysis of MnSS-2 after 3h PIII treated at 250°C, 380°C and 500°C a) XRD b) GXRD.*

It is difficult to distinguish nitrides from an expanded austenite lattice, as both of them are reported to exhibit similar crystal structure [28]. Further, the low scattering of N atom inhibits measurable intensities for the reflections of planes even if the crystal symmetry is changed. Hence in order to make it simple, the shift in the peak position is considered to be due to various metal-nitrogen stoichiometry of the phase, whether or not N addition leads to nitride formation or just an expanded austenite. Following this argument it is hypothesized that nitrogen implantation results in M_xN_y phase where M is a metal component of the alloy, x is the number of metal atoms, N is the nitrogen and y is the number of nitrogen atoms. The x/y ratio defines the number of metal atoms associated with each nitrogen atom (or stoichiometry of metal to nitrogen) and is reflected in the subsequent changes in lattice parameters or the peak positions in the XRD pattern. The advantage of such a method of analysis is that it enables suggesting the formation of nonstoichiometric phases. On examining the formula it can be said that x/y ratio can influence the lattice parameters in an inverse manner i.e. a decrease in the x/y ratio would increase the “a” value and hence the “d” value. This is primarily

because of the fact that any decrease in the x/y ratio is expected to cause an increase in the stoichiometry/ concentration of nitrogen per metal atom in M_xN_y. The increase in the nitrogen uptake results in increase in nitrogen concentration, which ultimately results in either expansion of existing austenite phase or formation of a new nitride phase. While such an analysis is made of the XRD patterns, where ever possible, attempt is made to relate the XRD data (lattice parameter) to known stiochiometry of the nitride phases reported in the literature.

As discussed earlier M represents the metal component of the alloy, here M may correspond to Fe or Mn or Ni or Cr or of combination of all [(FeNiMnCr)N]. But have been mostly reported as either mixed metal nitrides for the plane such as, $(Fe_3Ni)N$ or Fe_4N (x/y = 4) with d value 0.220 nm (JCPDS file no. 090318 for $(Fe_3Ni)N$ and JCPDS file no. 830875), (FeNi)N (x/y = 2) with d value 0.226 nm (JCPDS file no 140129) Fe_2N (x/y = 2) with 'd' values 0.210 nm(JCPDS file no 722126), and FeN (x/y = 1) with 'd' values 0.218 nm(JCPDS file no 031197) respectively. The above values are now compared with the'd' values of (111) of Type 304L SS specimen implanted at various temperatures for 3h to examine the type of nitrides formed. Thus, the d value of (111) at 250°C is 0.219 nm, and may corresponds to (Fe_3Ni) N of (111). Further increase in temperature to 380°C results in different d values for (111) plane i.e. d value 0.227 nm may correspond to (FeNi)N of (101) (d as per JCPDS file no 140129 is 0.225 nm) and the plane with d value 0.212 nm may correspond to Fe_2N. The GXRD of 250°C implanted sample doesn't show a well defined peak for nitrides as compared to that of the 380°C, but broadened peak near (111) plane shows the average d value near to 0.219 nm. Hence, the corresponding nitride peak (with d = 0.219 nm) was indexed as $(Fe_3Ni)N$. Accordingly it can be said that the phase structure changes from $(Fe_3Ni)N$ (at 250°C) to (FeNi)N plus and Fe_2N with increase in the temperature to 380°C.Finally at 500°C of implantation it forms (FeNi)N and/or FeN and α'. From the above discussion it can be said that nitrogen concentration in the "nitride phase" increases with increase in temperature. At low temperature (250°C) where diffusion of nitrogen is very low, hence nitride (Fe_3NiN) of less stoichiometry/concentration of N was formed with one nitrogen atom for each 4 metal atoms. At higher temperature for example 500°C, nitrides [(FeNi)N or FeN] of large stoichiometry/concentration of N was formed with one nitrogen atom for 2 metal atoms. This occurs mainly because of variation in the nitrogen diffusivity and reactivity at different temperatures. Possible compositions of nitrides in the specimens treated at various temperatures for 3h are summarized in Table 2. It is also to be noted that at higher implantation temperature, say 500°C,α′ is formed along with the nitrides, which was reported earlier as nitrogen induced bct phase [29, 30].

As regards to the amount of phases present on the surface, it was observed that on increasing the implantation temperature from 250°C to 500°C, there was a gradual increase in the relative intensity (I/I_0) of the (111) and (200) peaks in the conventional XRD patterns suggesting increase in the fraction of M_xN_y phase with temperature. This increase was accompanied by diminishing of the intensity of the original austenite peaks $(111)_\gamma$ and $(200)_\gamma$. The increase in percentage of I/I_0 with temperature, suggest that there is probably an increase in the thickness of the nitrogen enriched layer with increase in the temperature. Confirming the above discussion it is clear that at lower implantation temperature, say 250°C the nitride peaks is not clearly seen in XRD pattern, but it is clearly visible in GXRD spectra. At higher implantation temperature say 500°C nitride peaks were observed in both the spectra, suggesting thickness of the modified layer increases with increase in implantation temperature.

XRD and GXRD spectrum of untreated and 3h PIII treated MnSS-1 and MnSS-2 is also shown in Fig 2 and 3 respectively. It is clearly seen from the results that nitrogen when implanted at 250°C suppresses the ferrite peak and stabilizes the austenite phase. X-ray diffraction patterns obtained from the nitrogen implanted surfaces of both MnSS-1 and MnSS-2 alloys specimens show similar patterns, which are consistent with the one displayed by Type 304L SS. This indicates that identical M_xN_y phases where M may be Fe or Mn or Ni or Cr of combination of all [(FeNiMnCr) N].As discussed above in Type 304L SS, since only FeNi and Fe combination are seen in JCPDS files, so these peaks are indexed as $(Fe_3Ni)N$, Fe_2N, (FeNi)N.As seen in Type 304L SS, the transformed ferrite (α') also formed along with the M_xN_y phases. In MnSS-2 alloy, where there is no Ni, so M_xN_y phases can be combination of Fe, Mn and Cr. Hence M_xN_y phases were indexed as Fe_4N, Fe_2N and FeN. The main consideration is that the stiociometry of phases changes along with increase in treatment time and temperature. Possible phases present in the surface layers of the all the alloys treated at various temperatures for 3h are summarized in Table 2.

Table 2. *Possible phases predicted for 3h PIII treated alloys at different temperatures.*

Implantation temperatures	Identified phases		
	Type 304L SS	**MnSS-1**	**MnSS-2**
250°C	γ, M_xN_y (where M = FeNi or Fe and x = 4, y = 1) $(Fe_3Ni)N$, Fe_4	γ M_xN_y (where M = FeNi or Fe and x = 4, y = 1) $(Fe_3Ni)N$, or Fe_4N	γ M_xN_y (where M = Fe and x = 4, y = 1) Fe_4N
380°C	M_xN_y (where M = FeNi or Fe and x = 2, y = 1) Fe_2N M_xN_y (where M = FeNi or Fe and x = 2, y = 1) (FeNi)N	M_xN_y (where M = FeNi or Fe and x = 2, y = 1) (FeNi)N M_xN_y (where M = Fe or Ni and x = 2, y = 1) Fe_2N	M_xN_y (where M = Fe and x = 1, y = 1) FeN M_xN_y (where M = Fe and x = 2, y = 1) Fe_2N
500°C	M_xN_y (where M = FeNi or Fe) (FeNi)N (x = 2, y = 1) α'	M_xN_y (where M = FeNi or Fe) (FeNi)N (x = 2, y = 1) or FeN (x = 1, y = 1), α'	M_xN_y (where M = Fe and x = 1, y = 1) FeN α'

3.1.2. Effect of Implantation Duration

XRD and GXRD patterns of 6h PIII treated Type 304L SS is shown in Figure 4(a and b) the possible phases present in the surface layers are summarized in Table 3. On increasing time of nitrogen implantation from 3h to 6h for Type 304L SS, an undifferentiated broad peak was observed in the GXRD (Figure 4b) at 250°C near to (111) plane. This may again indicate high nitrogen activity at the surface and a steep nitrogen concentration profile from the surface of the alloy at longer interval of implantation because of slow diffusion of nitrogen at 250°C. With increase in implantation these peaks becomes sharper due to higher diffusion of nitrogen at higher temperatures. The existence of austenitic peaks in the XRD pattern at lower implantation temperatures (250°C and 380°C) for both 3h and 6h, indicate that increasing implantation time is not effective at these temperatures. Whereas, at higher implantation temperature (500°C) the increase in implantation time is more effective as it decreases the intensity (I/I_0) of α' peak. At this implantation condition (500°C, 6h) the diffusion of N is more and hence more stable nitride ((FeNi)N).

Table 3. *Possible phases predicted for 6h PIII treated alloys at different temperatures.*

Implantation temperatures	Identified phases		
	Type 304L SS	**MnSS-1**	**MnSS-2**
250°C	γ, M_xN_y (where M = FeNi or Fe and x = 4, y = 1) (Fe_3Ni)N, Fe_4N	γ M_xN_y (where M = FeNi or Fe and x = 4, y = 1) (Fe_3Ni)N, or Fe_4N	γ M_xN_y (where M = Fe and x = 4, y = 1) Fe_4N
380°C	M_xN_y (where M = FeNi or Fe and x = 2, y = 1) (FeNi)N	M_xN_y (where M = FeNi or Fe and x = 2, y = 1) (FeNi)N M_xN_y (where M = Fe or Ni and x = 2, y = 1) Fe_2N	M_xN_y (where M = Fe and x = 1, y = 1) FeN M_xN_y (where M = Fe and x = 2, y = 1) Fe_2N
500°C	M_xN_y (where M = FeNi or Fe) (FeNi)N(x = 2, y = 1)	M_xN_y (where M = FeNi or Fe) (FeNi)N(x = 2, y = 1) or FeN (x = 1, y = 1), M_xN_y (where M = Fe or Ni and x = 4, y = 1) Fe_3N	M_xN_y (where M = Fe and x = 1, y = 1) FeN

The XRD and GXRD patterns for Mn containing alloys (MnSS-1and MnSS-2) implanted for 6h (Fig 5 and 6) were consistent with those observed at 3h. As like Type 304L SS, the increase in implantation time is more effective only in higher implantation temperature (500°C). At higher implantation conditions (500°C, 6h), the diffusion of N is more and hence α' is completely eliminated by stabilizing the respective phases ie (FeNi)N for MnSS-1 and FeN for MnSS-2.

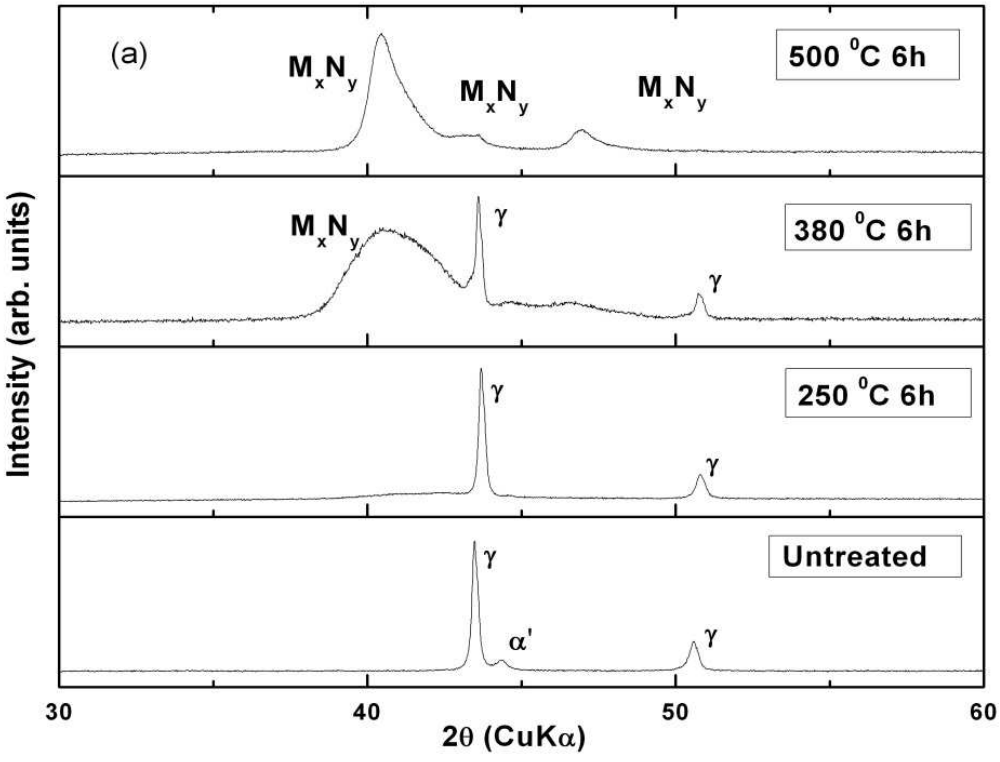

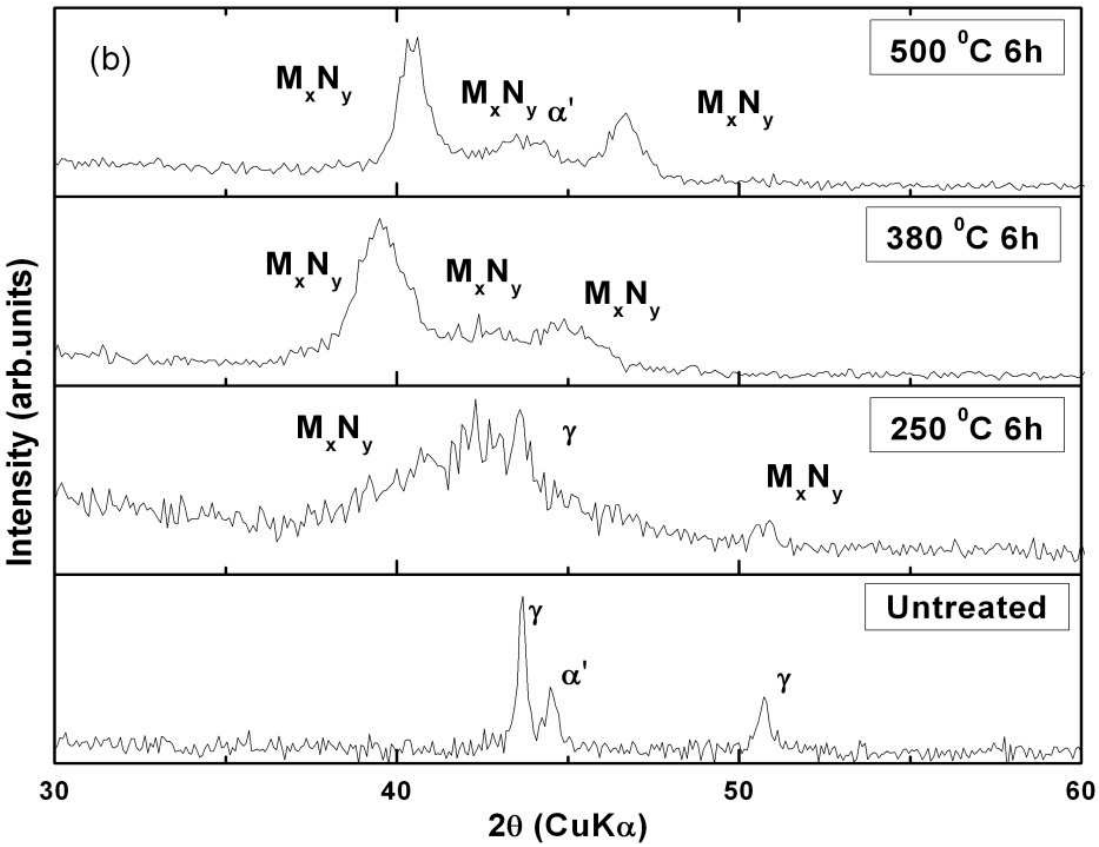

Figure 4. *Phase analysis of Type 304L SS after 6h PIII treated at 250°C, 380°Cand 500°Ca) XRD b) GXRD.*

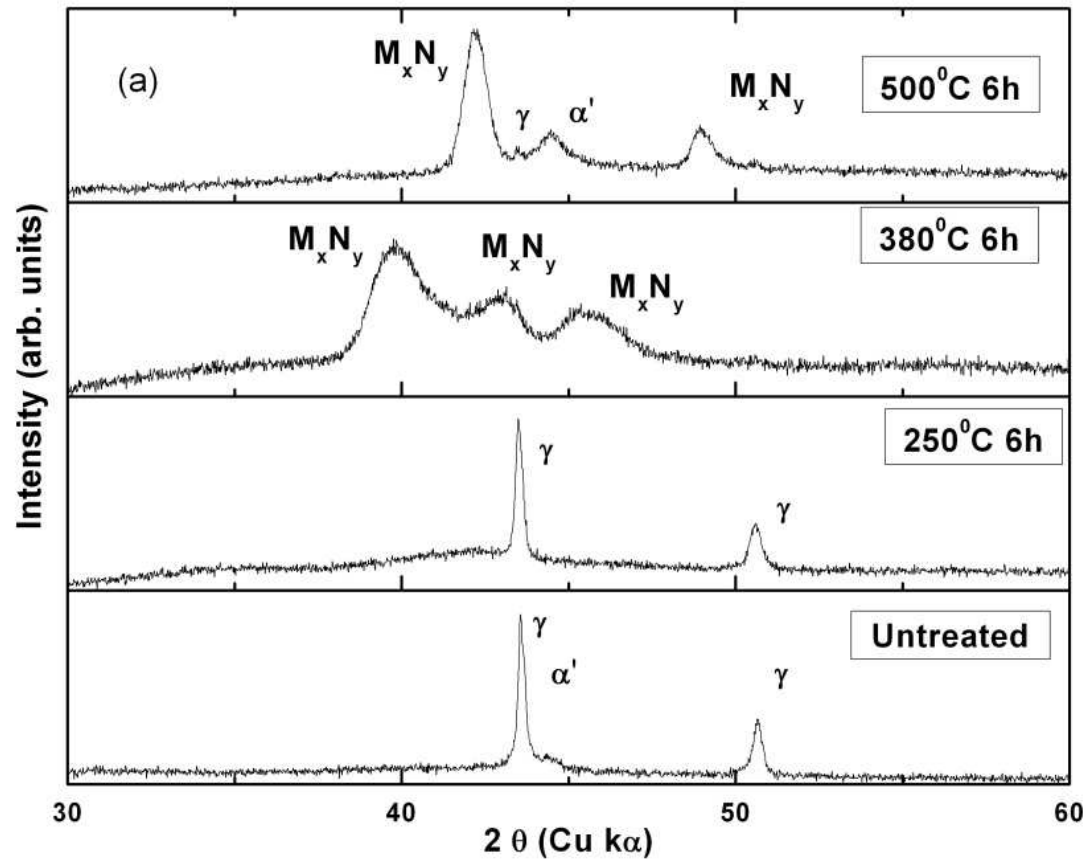

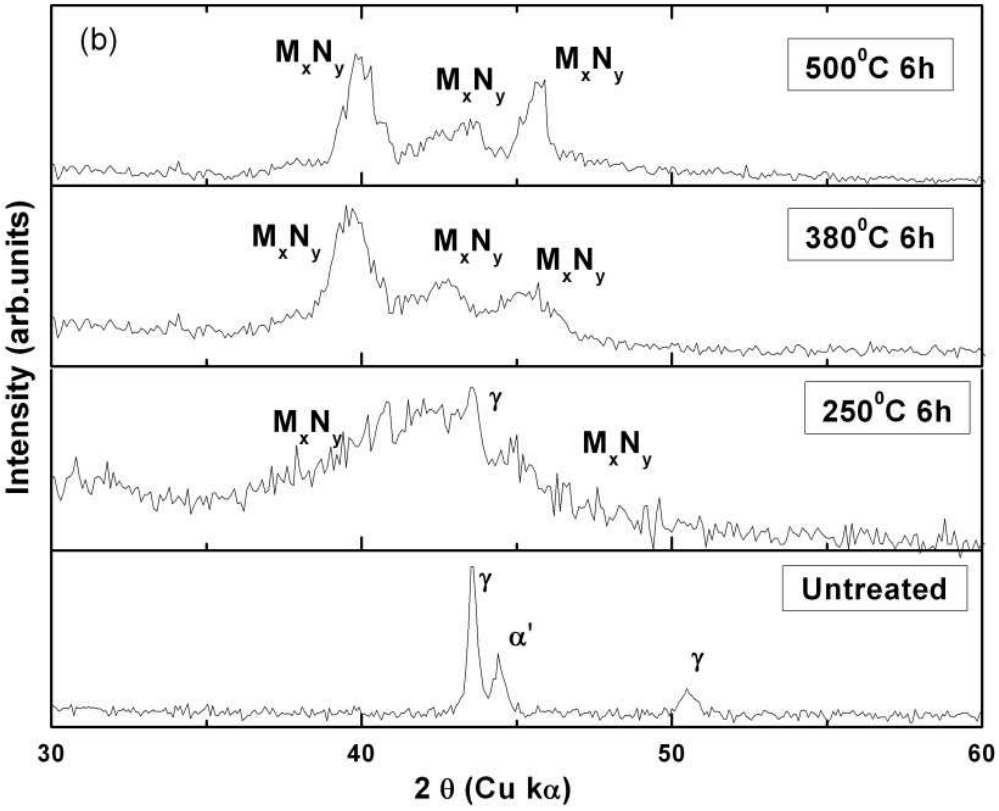

Figure 5. *Phase analysis of MnSS-1 after 6h PIII treated at 250°C, 380°Cand 500°Ca) XRD b) GXRD.*

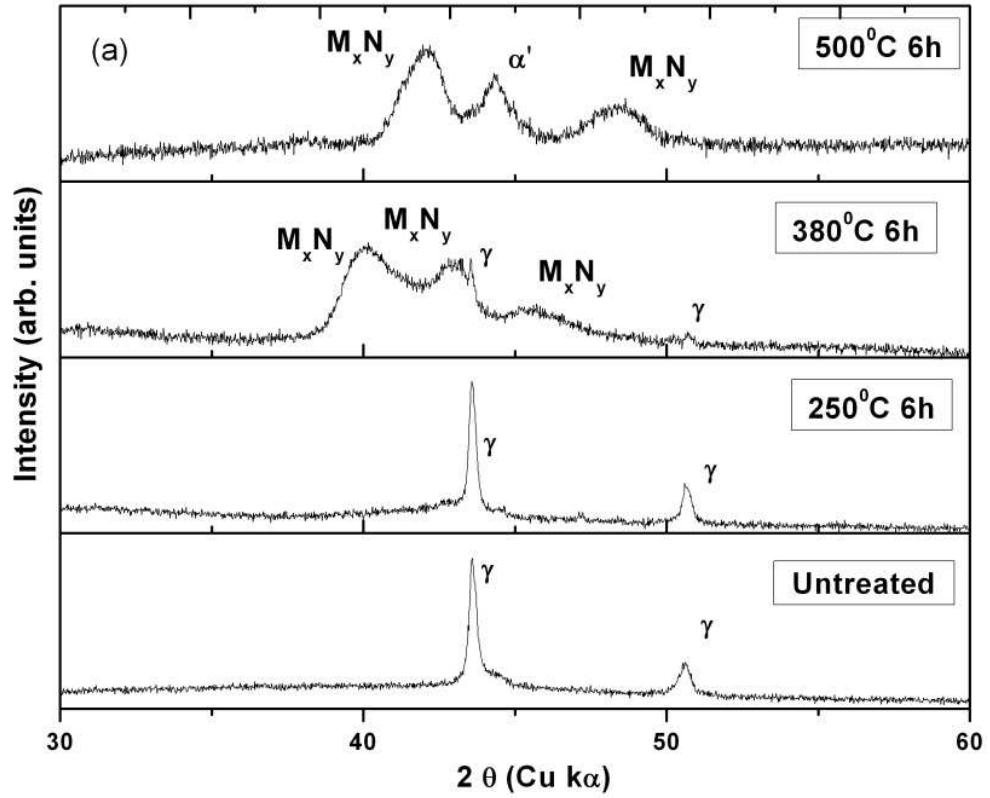

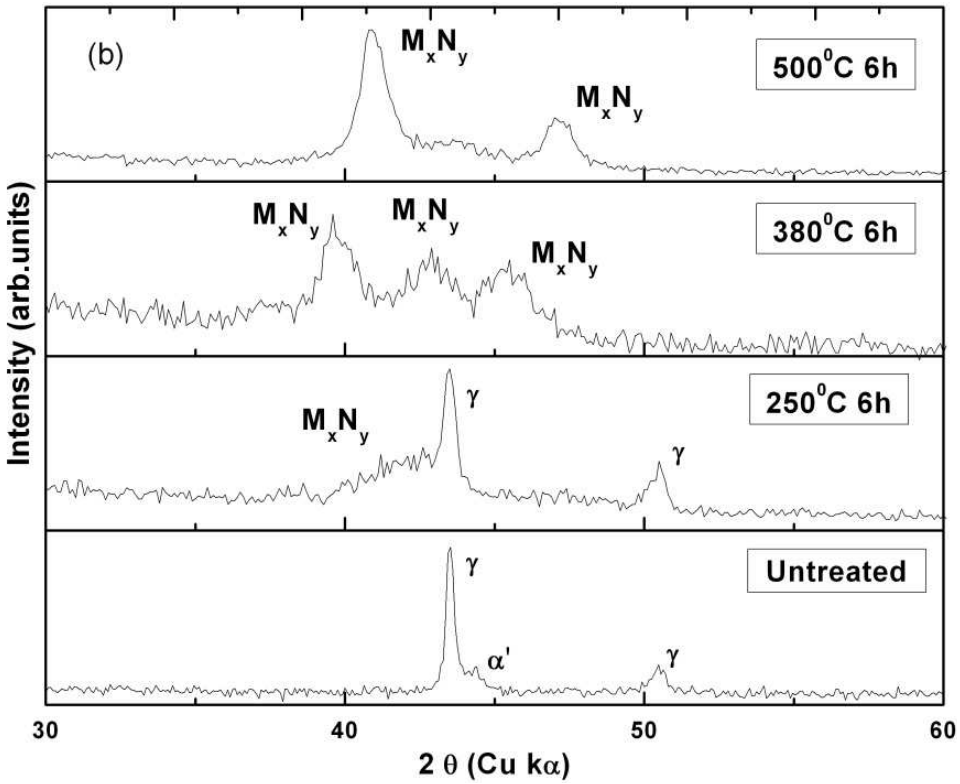

Figure 6. *Phase analysis of MnSS-2 after 6h PIII treated at 250°C, 380°Cand 500°Ca) XRD b) GXRD.*

3.2. Surface Hardness

Load dependent micro hardness measurements have been carried out on both untreated and the nitrogen ion implanted specimens of the three grades of austenitic stainless steels. Figure 7 shows the microhardness comparison of untreated and 3 h PIII treated alloys and Figure 8 for 6 h. The figure shows that the microhardness of the untreated alloy specimens varies in the range of 235–275 HV. It was also observed that under the given experimental range the effect of applied load on the microhardness of the untreated base alloy is insignificant, as almost constant values were obtained for hardness on increasing the applied load from 50 to 300 g.

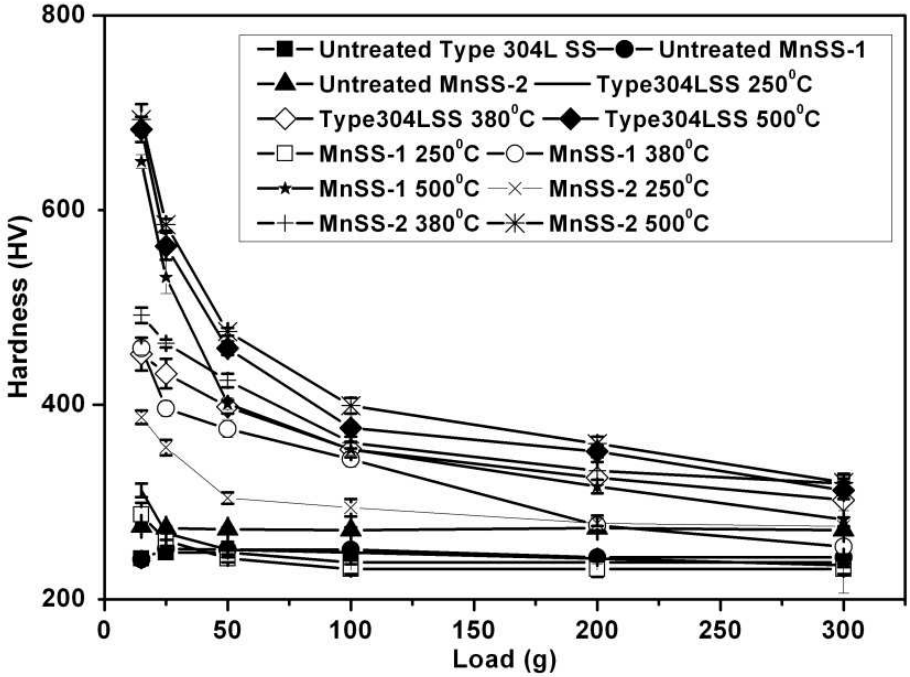

Figure 7. *Comparison of microhardness of untreated and 3h PIII treated Type 304L SS MnSS-1and MnSS-2.*

3.2.1. Effect of Implantation Temperature

Disparate the unimplanted specimens, the implanted ones were found to significantly on their hardness value with the applied load and temperature. Hence, hardness values are plotted in logarithmic scale to better represent a wide range of hardness variation exhibited by the specimens. From Figure 7it is clear that the implanted alloys exhibit significantly higher microhardness than that of the respective untreated condition. The graphs show that the implanted alloys exhibit a steep decrease in the hardness value at lower loads (25 to 100 g), and at higher loads hardness reduces gradually and attains the hardness closer to their respective substrate. It is to be pointed out that microhardness increases with increase in implantation temperature for all under investigation. It may be noted that the difference in the microhardness values obtained at 250°C and 380°C implantation temperatures was not significant and was very close to that of the substrate hardness (especially at higher loads),whereas, hardness increases substantially at 500°C.

The increase in hardness with increase in implantation temperature can be explained on the basis of the thickness of the surface implanted layers or the nitrogen concentration in the alloy matrix. During the implantation process there is a competition between the nitrogen build up at the surface and the nitrogen inward diffusion. At low temperature the diffusion is much slower hence a higher surface concentration is built up and a thin expanded austenite layer is obtained; this results in a low hardness value. At higher temperatures, the diffusion of nitrogen more and hence resulting a higher nitrogen concentration in austenite matrix leading to increase nitride layer (M_xN_y) thickness, which in turn resulting in higher hardness. These are consistent with the earlier studies [1, 20, 23] and also by above GXRD results, where I/I_0 increases with increase in implantation temperatures.

3.2.2. Effect of Implantation Duration

Variation of microhardness of the alloys with applied load for different implantation temperature at 6h implantation (Figure 8) was similar to that of 3h implanted conditions. However, alloys implanted at 6h shows higher microhardness than that of 3h implantation. The increase in the duration of implantation from 3h to 6h, increases diffusion of nitrogen in the austenite matrix. This leads to the increase in thickness of the nitride layer which ultimately results in a higher microhardness [1, 23]. These results are again consistent with the earlier GXRD studies, where I/I_0 increase with implantation duration.

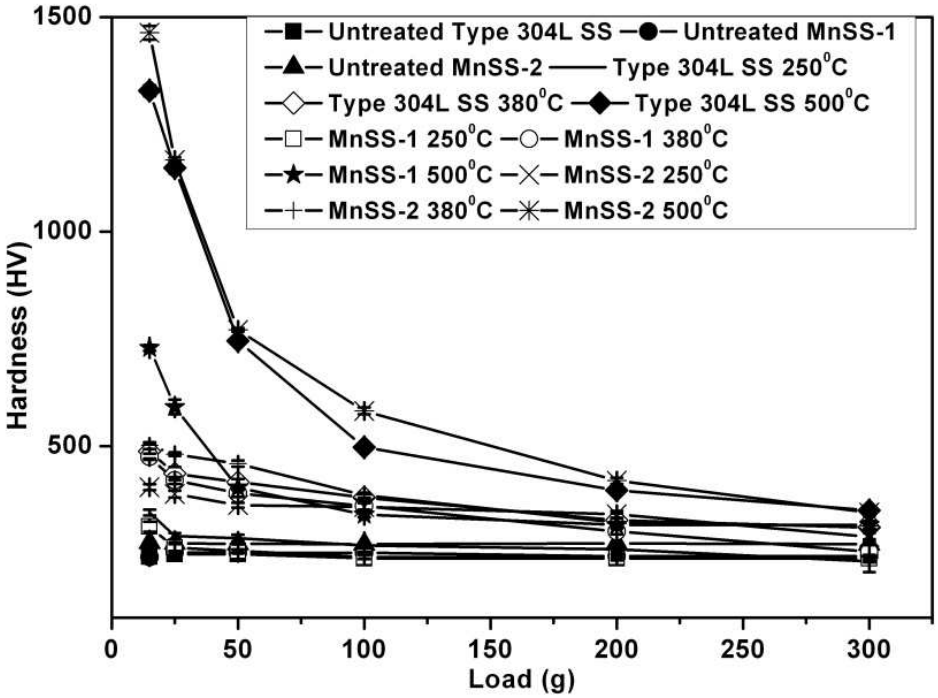

Figure 8. *Comparison of microhardness of untreated and 6h PIII treated Type 304L SS MnSS-1and MnSS-2.*

3.3. Effect of Alloying Element on Phase Formation and Surface Hardness

It is interesting study the effect of Mn on phase formation and surface hardness of the nitrogen implantation. If we compare the diffractrograms of all the alloys at 250°C 3h implanted condition, it is clear that there is no distinct nitride peak was observed in Ni free high Mn containing SS (MnSS-2), as compared to other Ni containing SS (Type 304L SS and Mn SS-1). On closer examination, it is clear that the relative intensity of the nitride peak is very low for lower Ni containing SS (MnSS-1) than that of higher Ni containing SS (Type 304L SS).This was confirmed by comparing the GXRD spectra (Figure 9b) of same treatment condition (250°C) for longer duration (6h), where γ and nitride peak was observed for MnSS-2 SS and only nitride peak was

observed in other two SS (304L SS and MnSS-1). Hence it can be said that nitrides are less favorable in Mn containing SS and more favourable in Ni containing SS. The nitrides are formed, when it exceeds the solubility of nitrogen in the matrix, this solubility limit in turn depends on the alloy composition [19]. Pehlke and co-workers [17] have given a relation for solubility limit of SS versus their alloying element in liquid steel (liquid solubility). They reported that Mn has positive effect in solubility of nitrogen, where as nickel has the negative effect, this was confirmed later by many researchers [31, 32]. The higher solubility of Mn containing steel can be confirmed by comparing the GXRD spectra of all the alloys at higher implantation temperatures, where Ni promotes the α′ formation and Mn suppress the α′ formation. Also from hardness studies it is evident that Ni free Mn containing steel (MnSS-2) showed higher hardness profile for all treatment conditions. This increase in hardness was mainly due to higher diffusion of nitrogen in Ni free Mn containing alloy matrix compared to that of Ni containing alloy (Type 304L and MnSS-1 SS). Hence it can be concluded that PIII treatment is more effective in Ni-free Mn containing SS (MnSS-2) with higher solubility of nitrogen increasing surface hardness than that of other two SS (Type 304L and MnSS-1).

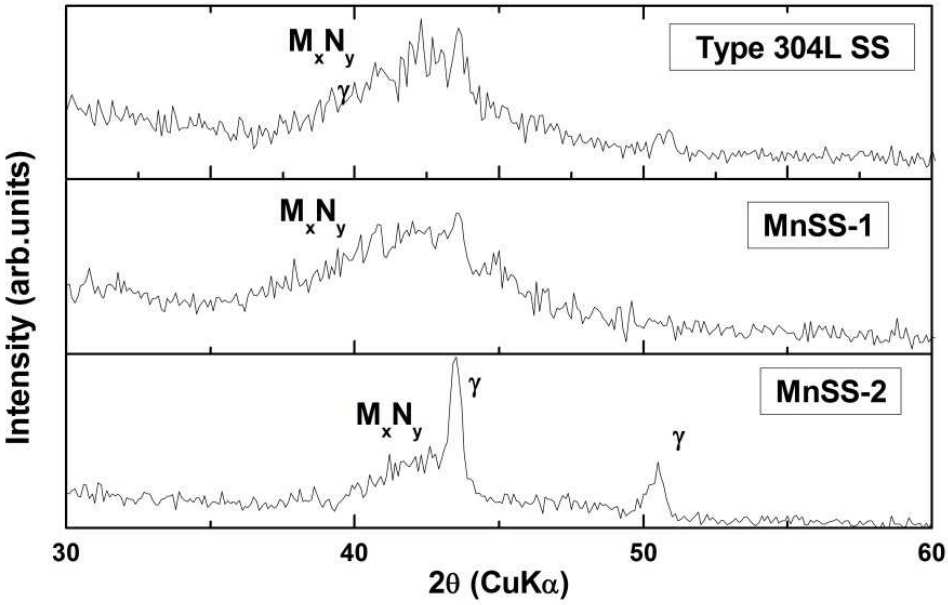

Figure 9. *Comparison of GXRD pattern of PIII treated alloys at 250°C for (a) 3h (b) 6h.*

4. Conclusion

The phase analysis carried out using XRD and GXRD techniques suggests that nitrogen ion implantation of various austenitic stainless steels, in general, results in the formation of either a solid solution of nitrogen or nitrides of different stoichiometry. Nitrogen concentration increases with increase in the treatment temperature (from 250 to 500°C).Surface hardness of both alloys has been found to increase with increasing treatment temperature and time. Ni-free Mn containing SS (MnSS-2) has higher solubility of nitrogen and higher surface hardness than that of other two SS (Type 304L and MnSS-1).

References

[1] W. Ensinger, Surface & Coating Technolology, 100-110 (1998) 341-352.

[2] Linda Gil, Sonia Brühl, Lorena Jiménez, Ovídio Leon, Rafael Guevara, Mariana and H. Staia, Surf. Coat. Technol. 201 (2006) 4424–4429.

[3] Xiubo Tian and Paul K. Chu, Scripta mater. 43 (2000) 417-422.

[4] P. Saravanan, V.S. Raja and S. Mukherjee, Surf. Coat. Technol.201 (1998) 8131-8135.

[5] Lei M. K. and Zhu X. M., Biomaterials,22 (2001) 641-647.

[6] J.R. Conrad, R.A. Dodd, F.J. Worzala, and X. Qiu, Surface & Coating Technolology, 36, (1988) 927-937.

[7] S. Mandl, D. Manova, H. Neumann, M.T. Pham, E. Richter, and B. Rauschenbach, Surf. Coat. Technol. 200 (2005) 104-108.

[8] L. Escalada, J. Lutz, S. Mändl, D. Manova, H. Neumann, and S. Simison, Surf. Coat. Technol.211 (2012) 76-79.

[9] Yanhui Zhao, Baohai Yu, Limin Dong, Hao Du, and Jinquan Xiao, Surf. Coat. Technol.210 (2012) 90-96.

[10] A. Fossati, F. Borgioli, E. Galvanetto, and T. Bacci, Corros. Sci.48 (2006) 1513–1527.

[11] K.S. Wang, H.L. Che, M.K. Lei, Surf. Coat. Technol.288 (2016) 30-35.

[12] M. CASTRO-COLIN, W. DURRER, J. A. LÓPEZ, E. RAMIREZ-HOMS, Journal of Iron and Steel Research, International, 23, 4, (2016), 380-384.

[13] Y. Li, Z. Wang, L. Wang, Applied Surface Science, 298, (2014), 243-250.

[14] D. Manova, S. Mändl, H. Neumann, B. Rauschenbach, Surf. Coat. Technol.256, (2014), 64-72.

[15] K. Ram Mohan Rao, S. Mukherjee, P.M. Raole, and I. Manna, Surf. Coat. Technol.200 (2005) 2049-2057.

[16] P. R. Levey, and A. Van Bennekom, Corrosion, 51 (1995) 911-921.

[17] R.D. Pehlke, and J.F. Elliatt, Transactions of Metallurgical Society of AIME, (1960) 218, 1088-1101.

[18] H. Pelletier, D. Muller, P. Mille, A. Cornet, and J.J. Grob Surf. Coat. Technol. 151 - 152 (2002) 377-382.

[19] Y. Li, L. Wang, J. Xu, and D. Zhang, Surf. Coat. Technol.206 (2012) 2430-2437.

[20] G.A. Collins, R. Hutchings, K.T. Short, J. Tendys, X. Li, and M. Samandi, Surf. Coat. Technol. 74-75 (1995) 417-424.

[21] J. Wang, J. Xiong, Q. Peng, H. Fan, Y. Wang, G. Li, and B. Shen, Mater. Charact. 60 (2009) 97-203.

[22] Y. Li, L. Wang, J. Xu, and D. Zhang, Surf. Coat. Technol.206 (2012) 2430-2437.

[23] M. Samandi, B. A Shedden, D. J. Smith, G. A.Collins, R. Hutchings and J. Tendys, Surface & Coatings Technology,59 (1993) 261-266.

[24] S. Mukherjee, J. Chakraborty, S. Gupta, P. M. Raole, P. I. John, K. R. M. Rao and I. Manna, Surface & Coating Technology, 156 (2002) 103-109.

[25] P.A. Dearnley, A. Namver, G. G. A. Hibberd and T. Bell, in: E. Broszeit, W.D. Munz, H. Oechsner, K.-T. Rie, G.K. Wolf (Eds.), Plasma Surface Engineering, vol. 1, DGM Informationsgesellschaft, Oberursel, "Proceedings of the 1st International Conference on Plasma Surface Engineering, Garmisch – Partenkirchen", 1989, p. 219. Vol 1 (1989) 219-226.

[26] K. Ichii, K. Fujimura and T. Takase, E. Broszeit, W.D. Munz, H. Oechsner, K.-T. Rie, G.K. Wolf(Eds.), Plasma Surface Engineering, vol. 1, DGM Informationsgesellschaft, Oberursel, "Proceedings of the 1st International Conference on Plasma Surface Engineering, Garmisch –Partenkirchen", (1989) 1187-1192.

[27] E. Menthe and K. T. Rie, Surface & Coatings Technology, 116-119 (1999) 199-204.

[28] D. J. Haen., C. Quaeyhaegens, G. Knuyt, L. De Schepper, L.M. Stals, and Van M. Stappen, Surface and Coating Technology, 60 (1993)468-473.

[29] F. Borgioli, A. Fossati, G. Matassini, E. Galvanetto, and T. Bacci, Surf. Coat. Technol. 204 (2010) 3410-3417.

[30] J. Talonen, and H. Hänninen, Acta Mater. 55, 18, (2007) 6108-18.

[31] N. Suutala, Metallurgical Transaction A, (1982) 13A, 2121-2130.

[32] C. Qiu, Metallurgical Transaction A, (1993) 24A, 629-645.